Journal of Rock Mechanics and Geotechnical Engineering 16 (2024) 588–596

Contents lists available at ScienceDirect

Journal of Rock Mechanics and Geotechnical Engineering

journal homepage: www.jrmge.cn

Full Length Article

A creep model for ultra-deep salt rock considering thermal-mechanical damage under triaxial stress conditions

Chao Liang [a], Jianfeng Liu [a,b,*], Jianxiong Yang [a], Huining Xu [a], Zhaowei Chen [c], Lina Ran [a,b]

[a] College of Water Resource and Hydropower, Sichuan University, Chengdu, 610065, China
[b] CNPC Key Laboratory of Oil and Gas Underground Storage Engineering, Langfang, 065007, China
[c] CNPC Engineering Technology R&D Company Limited, Beijing, 102206, China

ARTICLE INFO

Article history:
Received 16 December 2022
Received in revised form
15 May 2023
Accepted 15 June 2023
Available online 28 July 2023

Keywords:
Creep experiments
Creep model
Thermal and mechanical damage
Fractional derivative

ABSTRACT

To investigate the specific creep behavior of ultra-deep buried salt during oil and gas exploitation, a set of triaxial creep experiments was conducted at elevated temperatures with constant axial pressure and unloading confining pressure conditions. Experimental results show that the salt sample deforms more significantly with the increase of applied temperature and deviatoric loading. The accelerated creep phase is not occurring until the applied temperature reaches 130 °C, and higher temperature is beneficial to the occurrence of accelerated creep. To describe the specific creep behavior, a novel three-dimensional (3D) creep constitutive model is developed that incorporates the thermal and mechanical variables into mechanical elements. Subsequently, the standard particle swarm optimization (SPSO) method is adopted to fit the experimental data, and the sensibility of key model parameters is analyzed to further illustrate the model function. As a result, the model can accurately predict the creep behavior of salt under the coupled thermo-mechanical effect in deep-buried condition. Based on the research results, the creep mechanical behavior of wellbore shrinkage is predicted in deep drilling projects crossing salt layer, which has practical implications for deep rock mechanics problems.

1. Introduction

Salt rock is a chemical evaporite that has low permeability, low porosity, and good self-healing abilities. Thanks to these favorable properties, salt rock is not only investigated as a natural gas/oil reservoir, as well as an internationally recognized ideal repository medium for high-level radioactive waste (HLW) (Xie et al., 2011; Zhou et al., 2011). With the exploitation of oil and gas resources going deep into the earth, rheological deformation of drilling wellbore plays a crucial role in the stability of deep formation (Taheri et al., 2020). During the drilling process, the in situ formation stress is disturbed, and the stress dissipation due to unloading is required to be balanced by supporting stress. However, the wellbore surrounding rock is still in an under-balanced state at the same time, even taking the artificial supporting measures (Cheng et al., 2019; Wang et al., 2021). Furthermore, the time-effect of deep energy exploitation may lead to the rheological salt rock deformation, which poses potential threats on the instability of wellbore. Therefore, in order to safely operate deep energy exploration and to maximize economic benefits, it is imperative to study the creep behavior of deep-buried salt rock.

Unlike most of the pure salt rock in other countries, the salt rock in China contains a lot of impurities, the composition of which is complicated (Xi et al., 2007, 2008; Wu et al., 2017). Zhang et al. (2014) revealed the periodicity of sequence sedimentation characteristics of interlayered salt through studying its rhythm, lithology and mechanical characteristics. Field investigations and laboratory experiments show that chemical sedimentation interfaces are stronger than mechanical sedimentation interfaces. In view of the specific characteristics of salt rock containing impurity, many scholars had studied the creep mechanical properties. For example, Xi et al. (2007) conducted a long-term uniaxial creep experiment of salt rocks with different material compositions, where the creep rate of layered salt rocks is found to be closely related to their composition and structure. To investigate the creep deformation of different rock types, Tang et al. (2010) conducted

* Corresponding author. College of Water Resource and Hydropower, Sichuan University. Chengdu, 610065, China.
E-mail address: liujf@scu.edu.cn (J. Liu).

Peer review under responsibility of Institute of Rock and Soil Mechanics, Chinese Academy of Sciences.

https://doi.org/10.1016/j.jrmge.2023.06.009

triaxial creep experiments of salt rock, mudstone, and interlayers of salt rock and mudstone, where the creep rates of salt-mudstone interlayer were proved to be lower than salt rocks and larger than mudstones under the same stress conditions. To investigate the influence of confining pressure and impurity on hydro-mechanical behavior of salt rock, Zhang et al. (2020) carried out triaxial compression experiments accompanied with permeability test on impurity salt rock samples. According to the results, the confining pressure has a positive effect on triaxial compressive strength and has a negative effect on fluid seepage. For the impurity of salt rock, higher impurity contents are accompanied by greater bearing capacity and larger permeability.

In the creep deformation process, the creep strain state at a certain timing is related both to the current stress state as well as to the whole stress history prior to the current moment (Wu et al., 2020a). In order to accurately describe the time-dependent effect of creep deformation and its dependence on stress history, fractional order is an effective tool for establishing creep constitutive models, which is widely adopted by many researchers (Chen et al., 2013; Peng et al., 2018). Besides, Zhou et al. (2011, 2013) proposed a fractional creep constitutive model by replacing the Newtonian dashpot with an Abel dashpot in the Nishihara model. The new model is proved to be more accurate when it comes to describing salt rock creep behavior at the elastic-plastic transition stage. On the basis of numerous long-term laboratory creep experiments of salt rock, Wu et al. (2020a, b, 2022) proposed nonlinear fractional-order and variable-based fractional-order models, where the accelerated creep behavior of salt rock can be better represented by the improved model.

High geo-temperature and geo-stress co-exist in deep-buried environment (Xie et al., 2015), where the deformation of rock mass after unloading is closely associated with time and showing obvious rheological characteristics, which pose certain technical challenges to deep engineering projects (Dusseault et al., 2004; Tao et al., 2020; Xu et al., 2020). A large number of researchers have studied the effect of high temperature and high stress on the mechanical properties of rock (Hu et al., 2009; Blanco-Martín et al., 2016; Kumari et al., 2017; Yang et al., 2017; Chen et al., 2019; Cai et al., 2021; Feng et al., 2021; Lyu et al., 2022). For example, Wang et al. (2015, 2020) proposed an attenuating fractional-order model by introducing a stress-based creep function into the ordinary fractional-order viscoelastic constitutive relation of viscous body, where the viscosity coefficient decays with stress and time. As a result, the entire creep process of rock was represented by a four-element non-linear viscoelastic-plastic creep model. Chen et al. (2014) introduced the temperature variable into the Nishihara model and replaced the element describing the accelerating stage with an Abel dashpot. The modified model is capable of describing the entire creep process of granite under various temperature conditions. Additionally, the relative simplicity of model formulation makes it easier to be applied to practical engineering problems.

To further investigate the influence of ultra-high temperature and pressure on creep behaviors of deep impurity salt, a creep constitutive model based on laboratory experimental phenomena is presented in this paper. Considering the unloading stress state in the drilling process, a set of triaxial creep experiments was conducted at five elevated temperatures with axial pressure constant and confining pressure unloaded condition. A three-dimensional (3D) fractional order derivative creep model is developed based on the thermal and mechanical damage theory, which well reproduces the creep deformation process. In addition, the key model parameters are determined and analyzed in detail. The study not only reveals the creep mechanism of deep buried impurity salt rock under high temperature and unloading conditions, but also provides certain theoretical basis and deformation prediction scheme for wellbore stability of oil and gas drilling engineering.

2. Specimen preparation and experimental procedure

2.1. Physical properties of deep salt

The impurity salt rocks used in this study were obtained from a certain deep drilling project in China. As shown in Fig. 1, the samples are reddish-brown, cylinder-shaped, and 50 mm in diameter and 100 mm in height, which are processed through indoor dry drilling method according to the standard recommend by International Society for Rock Mechanics and Rock Engineering (Feng et al., 2019). Through X-ray diffraction (XRD) analysis (Fig. 2), the specimen is mainly composed of NaCl and contains impurities such as SiO_2 and Fe_3O_4. The average natural density is 2.07 g/cm^3. Listed below are the basic physical parameters of the samples (Table 1).

2.2. Experimental setting and procedure

2.2.1. Temperature and stress path

Maintaining wellbore stability during drilling is a crucial problem in engineering, and wellbore instability is the main factor that restricts the development of deep drilling engineering. In the drilling engineering, high-pressure drilling fluid column pressure is usually used to balance the stress released by drilling before cementing. However, due to ultra-high geo-stress, there is often a differential pressure between the column and the formation, and the wellbore wall is still in an “under-balanced stress” state after unloading. To investigate the creep mechanism of deep salt under such condition, a constant axial pressure coupled with unloading confining pressure is adopted in the creep experiments. In addition to high geo-stress in deep-buried condition, high geo-temperature also exists. The coupling effect of high geo-stress and geo-temperature poses a severe technical challenge to deep drilling engineering. To study the creep mechanical behaviors of impurity rock salt under coupled thermal-mechanical condition, the axial pressure in the experiments is fixed to 125 MPa, and the temperatures are set to 100 °C, 110 °C, 120 °C, 130 °C and 140 °C, respectively, according to the geological data obtained in the field.

2.2.2. Experimental procedure

The experiments were performed using MTS 815 Flex GT (Fig. 3), rock mechanics system in Sichuan University. The maximum load capacity of the experiment system is 4600 kN, maximum confining pressure is 140 MPa, and maximum temperature is 200 °C. The range of the axial and radial extensometer is 0–50 mm and −2.5–12.5 mm, respectively (Fig. 4). Following is the description of the experimental procedures: (i) Increasing the confining pressure to 10 MPa; (ii) Heating the triaxial compression cell to the set temperature; (iii) Increasing the confining pressure to 120 MPa,

Fig. 1. Impurity salt rock specimens.

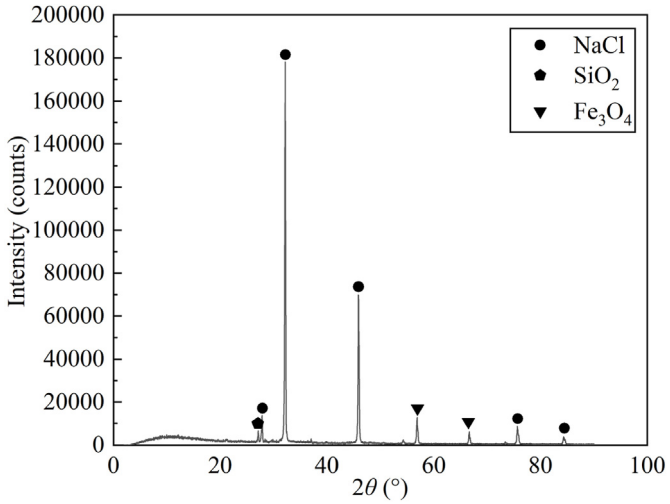

Fig. 2. The XRD pattern of impurity salt rock.

and then deviatoric stress is set to 5 MPa; (iv) Maintaining the deviatoric stress at 5 MPa for 3 h; and (v) Maintaining the axial stress at 125 MPa, while unloading the confining pressure stage by stage at an interval of 5 MPa.

3. Experimental results

3.1. Creep deformation

As shown in Fig. 5, all creep axial strain duration curves were compared. The overall slope of creep duration curves increases as the temperature rises. In response to the increase in temperature, the accelerated creep appears earlier. Under 130 °C and 140 °C conditions, the accelerated creep of specimen occurs at the fifth and fourth stages, respectively. There are several reasons for this phenomenon. The grain structure of salt rock at high temperature is changed by the dislocation slip and extrusion after thermal expansion. As the temperature rises, the minerals of the rock components undergo greater thermal expansion. Similarly, the thermal expansion coefficient of impurity mineral grains in rock differs from that of salt crystal, and the thermal expansion deformation between different grain boundaries lacks of homogeneity, resulting in more frequent thermal extrusion and dislocation. Under certain high temperature conditions, deterioration of mechanical properties occurs in rock samples, which will promote the deformation of rock with the accumulation of damage, and eventually further transform into accelerated creep (Yang et al., 2020; Yang and Fall 2021). Fig. 6 compares the time when the radial and axial strain reach 6.3% (10 mm of radial displacement) respectively at each temperature condition. To reach 6.3% strain value, the strain in radial direction requires longer time than the strain in axial direction at various temperatures, and its average multiple is 1.63. The time needed to reach 6.3% strain shortens as temperature increases, which proves once again that the specimen deformation accelerates as the temperature rises.

In creep experiments, transient strain and creep strain can be found. As an important component of rock creep deformation, the creep strain needs to be further analyzed and quantified. Fig. 7 shows the creep strain ratios of impurity salt rocks at different deviatoric stresses and temperatures. In this case, it is evidenced that the creep strain ratios of impurity salt rocks at different levels are all greater than 84.7%, and going up with the increase in temperature and deviating stresses within the range of 84.7%–97.5%. The variation range of creep strain ratio under different deviatoric stress decreases as the temperature rises. Taking temperature 120 °C and deviatoric stress 10 MPa as critical points. As seen from the green box and yellow box, the ratio variation range is 9.2% and 3.7%, respectively. It indicates that when the temperature and the deviatoric stress exceed 120 °C and 10 MPa respectively, there is a gradual weakening of the impact of these two changes on creep strain ratio, which shows the importance of the creep strain of impurity salt rock in its overall deformation. A detailed study of temperature and deviatoric stress effects on rock mechanical properties in creep stage is further studied under experimental conditions in the following part.

In Fig. 8, equations were fitted to describe the variation of steady-state creep rate with deviatoric stress at different temperatures, where the function shows a good fitting, with average R^2 of 0.99. Under the temperature condition of 100 °C and 120 °C, linear functions can be used to express the steady-state creep rate as the deviatoric stress increases, and the slope of each linear function becomes larger as the temperature rises, indicating that the crucial role of temperature in promoting the creep deformation of impurity salt rock. When the temperature exceeds 130 °C, the steady-state creep rate increases exponentially as the deviatoric stress increases, with speeding up evolution trend for elevated temperatures. This also explains the phenomenon of which the accelerated creep occurs at $T = 130$ °C, σ_1-$\sigma_3 = 25$ MPa and $T = 140$ °C, σ_1-$\sigma_3 = 20$ MPa from the point of view of creep rate, that is, the larger the steady-state creep rate is, the more the cumulative deformation of the specimen will have. When this deformation reaches a certain value, the rock structure becomes unstable. Consequently, as the applied temperature is higher, the rock will enter into the accelerated creep deformation stage.

3.2. Destruction form

In the creep experiments of the impurity salt rock, both samples showed accelerated creep stage at 130 °C and 140 °C. However, in order to prevent the damage of the experiment equipment caused by sudden failure of samples during the experiment, the test had to be stopped immediately once the upward trend appeared in the real-time displacement data graph. Hence, although all of the impurity salt rocks undergo the accelerated creep stage under the above conditions, they retain similar morphology after compression.

As can be seen from the compressed end face of specimen in Fig. 9a, all of the samples have a few gaps on their end faces. This is because the size of impurity grain and salt grain is different and the cohesion between them is not firm. Therefore, in the compression process, faces on each end are protruded, and the protruding parts are uneven. A high temperature will cause the rock mineral grains to expand, increasing its deformation. From the overall shape of the compressed impurity salt rocks in Fig. 9b, the destruction morphology presents a kind of drum with small diameter at both ends and large diameter in the middle, and the depression deformation at both ends become deeper with the increase of temperature.

4. Establishment of creep-damage model

4.1. Thermal damage variable and mechanical damage variable

High temperature conditions exist in deep environment, and numerous researches have proved that mechanical properties of rocks vary greatly between room temperature and high temperature conditions, e.g. Poisson's ratio, yield strength, elastic modulus, and viscosity (Wang et al., 2019; Zhang et al., 2021; Lyu et al., 2022).

Table 1
Basic information of samples in creep experiments.

Specimen	Height (mm)	Diameter (mm)	Mass (g)	Density (g/cm^3)
NY-1	99.85	49.92	407.15	2.08
NY-2	99.98	49.9	404.35	2.07
NY-3	99.91	49.93	403.75	2.06
NY-4	100.13	49.93	408.87	2.09
NY-5	99.92	49.95	406.18	2.07

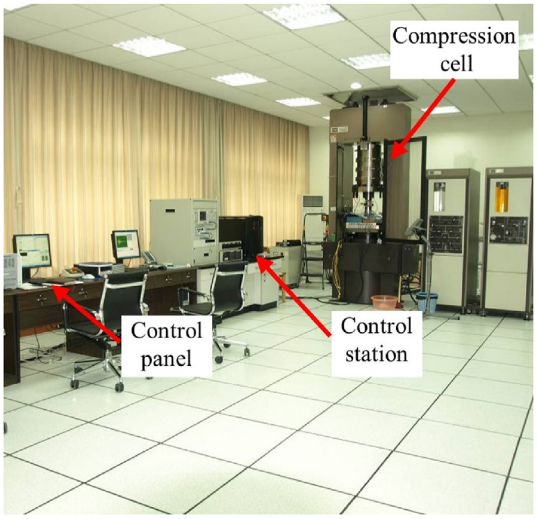

Fig. 3. Experiment equipment.

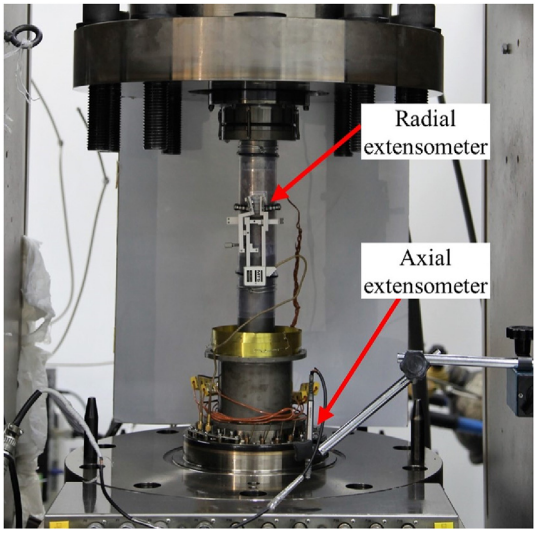

Fig. 4. Experiment platform.

When salt rock mineral particles are subjected to high temperatures, their morphology changes because of NaCl grain expansion and softening, accompanied by the transformation of mechanical properties of salt rocks to ductility (Soppe et al., 1994; De Las Cuevas, 1997; Li et al., 2018). In order to better understand how temperature influences the rock mechanical properties and how mechanical properties vary with temperature, many scholars have studied this behavior by introducing the temperature damage variables into the constitutive equation. In the analysis focusing on the influence of temperature on the basic mechanical parameters, researchers found that the damage variable is in a negative exponent relationship with temperature (Zhu et al., 2011; Zhang et al., 2022). The following thermal damage factor D_T can be deduced based on the above statements:

$$D_T = 1 - \alpha \exp(-\beta \Delta T) \quad (0 \le D_T \le 1) \tag{1}$$

where α and β are the constants affected by temperature; ΔT is the difference between room temperature and experimental temperature, and the room temperature is 26 °C in this study.

In addition to thermal damage, the mechanical damage (D_M), defined by the loading damage accumulation, is also of concern. Microcracks within the rock is closed and reopened repeatedly during the loading process, resulting in continuous damage. Subsequently, the microcracks propagate and coalescence to create larger cracks (Xu and Karakus, 2018). As a result, the creep will enter into accelerated creep stage when the deformation reaches a certain value and the stress reaches its yield limit. In this case, the structural stability of the stable rock changes and the damping of viscosity coefficient should consider the damage effect of thermal and mechanical coupling. In light of a salt creep experiment, Zhou et al. (2013) assumed that the mechanical damage of the impurity salt in deep condition conforms to a negative exponential function, which is adopted in the study as follows:

$$D_M = 1 - e^{-\omega t} \quad (0 \le D_M \le 1) \tag{2}$$

where ω is the viscosity coefficient, s^{-1}; and t is the creep time, s.

4.2. A new creep constitutive model based on damage variables

The creep process is consisted of three stages: the initial transient stage, steady stage, and accelerated stage. It could be expressed in the following function:

$$\varepsilon = \varepsilon_e + \varepsilon_{ve} + \varepsilon_{vp} \tag{3}$$

where ε is the total strain; ε_e is the transient strain; ε_{ve} is the steady stage strain; and ε_{vp} is the accelerated stage strain.

To accurately characterize the three creep stages, two mechanical elements are used, namely Hooke's body and Abel dashpot, as shown in Fig. 10.

Based on the assumption that the damage variable affects the rock mechanical properties, we assume that thermal damage exists at the initial and steady stages, and that both thermal and

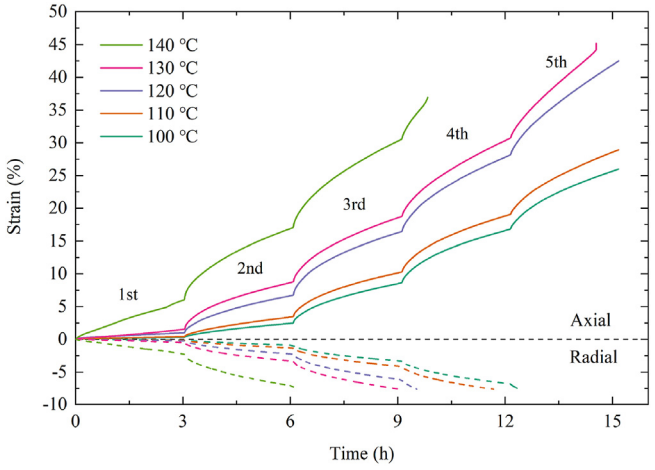

Fig. 5. Creep curves under different temperatures.

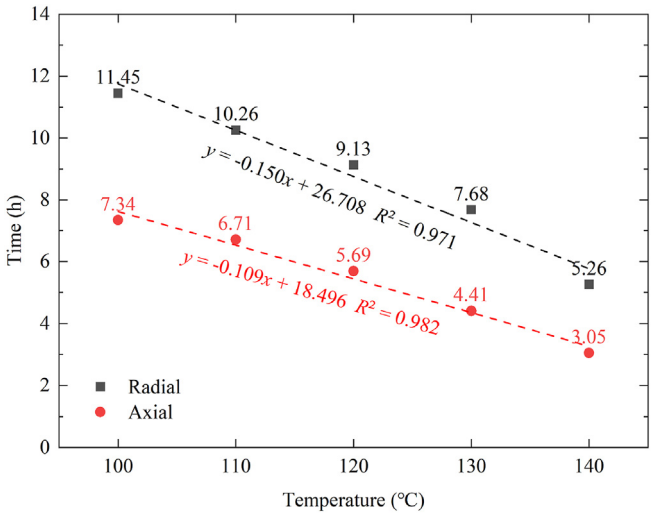

Fig. 6. Comparison of axial and radial strain reaching 6.3% at different temperatures.

mechanical damage exist at the accelerated stage. Fig. 11 shows the three types of modified mechanical elements.

With respect to temperature, the constitutive relationship of the Hooke's body can be reconstructed as follows:

$$\varepsilon_{\mathrm{e}} = \frac{\sigma_0}{E(T)} \tag{4}$$

$$E(T) = E_0(1 - D_{\mathrm{T}}) \tag{5}$$

where $E(T)$ is the elastic modulus considering the effect of temperature T, GPa; and σ_0 is the stress of the Hooke's body, MPa.

For the first Abel dashpot, higher temperature causes thermal damage, and as a result leading to coefficient attenuation (Liang et al., 2022). Eq. (6) gives the constitutive relation of Abel dashpot. By using Riemann-Liouville transformation and incorporating thermal damage, the constitutive relationship of the first Abel dashpot is expressed as

$$\sigma_1 = \eta_0 \frac{\mathrm{d}^{\gamma}\varepsilon_{\mathrm{ve}}(t)}{\mathrm{d}t^{\gamma}} \quad (0 \le \gamma \le 1) \tag{6}$$

$$\varepsilon_{\mathrm{ve}} = \frac{\sigma_1}{\eta_0(T)} \frac{t^{\gamma}}{\Gamma(\gamma+1)} \quad (0 \le \gamma \le 1) \tag{7}$$

$$\eta_0(T) = \eta_0(1 - D_{\mathrm{T}}) \tag{8}$$

where σ_1 is the stress of the first Abel dashpot, MPa; $\eta_0(T)$ is the viscosity coefficient at temperature T, GPa s^{γ}; Γ is Gamma Function; and γ is the fractional derivative order.

The creep will enter into accelerated creep stage when the deformation reaches a certain value (ε_{s}). This stage can be expressed by the second Abel dashpot, which takes into account the coupling of thermal and mechanical damage. The damage variable D_{TM} is utilized for characterizing the degradation of the viscosity coefficient caused by thermal and external stress, leading to the derivation of the subsequent expression:

$$D_{\mathrm{TM}} = D_{\mathrm{T}} + D_{\mathrm{M}} - D_{\mathrm{T}}D_{\mathrm{M}} \tag{9}$$

$$\varepsilon_{\mathrm{vp}} = \frac{\sigma_2}{\eta_1(T,\sigma)} \frac{{t_1}^{\gamma}}{\Gamma(\gamma+1)} \quad (0 \le \gamma \le 1) \tag{10}$$

$$\eta_1(T,\sigma) = \eta_1(1 - D_{\mathrm{TM}}) \tag{11}$$

$$t_1 = t - t_0 \tag{12}$$

where σ_2 is the stress of the second Abel dashpot, MPa; $\eta_1(T,\sigma)$ is the viscosity coefficient affected by thermal–mechanical damage, GPa s^{γ}; t_1 is the accelerated creep stage duration, s; and t_0 is the moment that enters the accelerated creep stage, s.

Combination of two modified Abel dashpots and one improved Hooke's body is able to form a new creep model (see Fig. 12), where the total strain is given by the combination of Eq. (4), Eq. (7) and Eq. (10):

$$\varepsilon = \begin{cases} \dfrac{\sigma}{E(T)} + \dfrac{\sigma}{\eta_0(T)} \dfrac{t^{\gamma}}{\Gamma(\gamma+1)} & (\varepsilon < \varepsilon_{\mathrm{s}}) \\ \dfrac{\sigma}{E(T)} + \dfrac{\sigma}{\eta_0(T)} \dfrac{t^{\gamma}}{\Gamma(\gamma+1)} + \dfrac{\sigma}{\eta_1(T,\sigma)} \dfrac{{t_1}^{\gamma}}{\Gamma(\gamma+1)} & (\varepsilon \ge \varepsilon_{\mathrm{s}}) \end{cases} \tag{13}$$

4.3. Triaxial creep-damage constitutive model

In deep drilling project, ultra-high stress and temperature will affect the stabilization of the surrounding rock, and the rock is subjected to 3D stress loading (Dusseault et al., 2004). To accurately describe the creep mechanical behavior, the creep constitutive model should take into account three dimensions. The 3D form of the creep constitutive model can be deduced similar to an analogy in its one dimensional form (Wu et al., 2021). According to the 3D constitutive model, the total strain is

$$\varepsilon_{ij} = \varepsilon_{ij}^{\mathrm{e}} + \varepsilon_{ij}^{\mathrm{ve}} + \varepsilon_{ij}^{\mathrm{vp}} \tag{14}$$

where ε_{ij} is the total effective deviatoric strain tensor; $\varepsilon_{ij}^{\mathrm{e}}$ is the effective deviatoric strain tensor of Hooke's body; $\varepsilon_{ij}^{\mathrm{ve}}$ is the effective deviatoric strain tensor of the first Abel dashpot; and $\varepsilon_{ij}^{\mathrm{vp}}$ is the effective deviatoric strain tensor of the second Abel dashpot.

Under the 3D stress state, the stress tensor σ_{ij} and the strain tensor ε_{ij} can be decomposed as follows:

$$\left.\begin{aligned} \sigma_{ij} &= S_{ij} + \delta_{ij}\sigma_{\mathrm{m}} \\ \sigma_{\mathrm{m}} &= \frac{1}{3}(\sigma_1 + \sigma_2 + \sigma_3) \end{aligned}\right\} \tag{15}$$

$$\left.\begin{aligned} \varepsilon_{ij} &= e_{ij} + \delta_{ij}\varepsilon_{\mathrm{m}} \\ \varepsilon_{\mathrm{m}} &= \frac{1}{3}(\varepsilon_1 + \varepsilon_2 + \varepsilon_3) \end{aligned}\right\} \tag{16}$$

where δ_{ij} is the Kronecker function.

In generalized Hooke's law, Hooke's body has the following 3D constitutive relationship:

$$\left.\begin{aligned} S_{ij} &= 2G(T)e_{ij} \\ \sigma_{\mathrm{m}} &= 3K(T)\varepsilon_{\mathrm{m}} \end{aligned}\right\} \tag{17}$$

where $K(T)$ is the bulk modulus considering the effect of temperature T, GPa; $G(T)$ is the shear modulus considering the effect of temperature T, GPa.

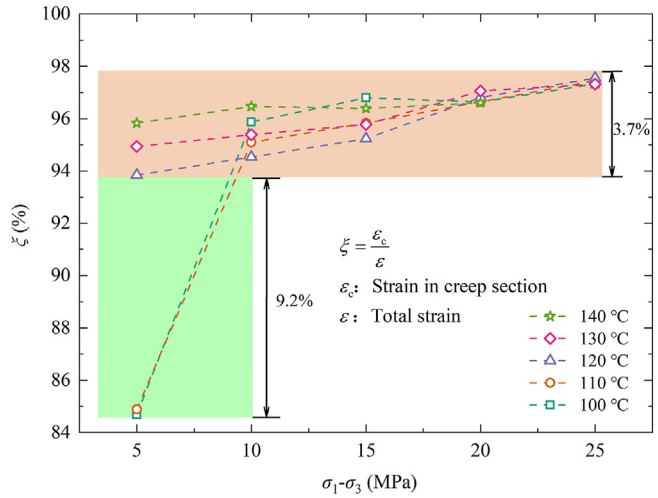

Fig. 7. Proportion of creep section at different conditions.

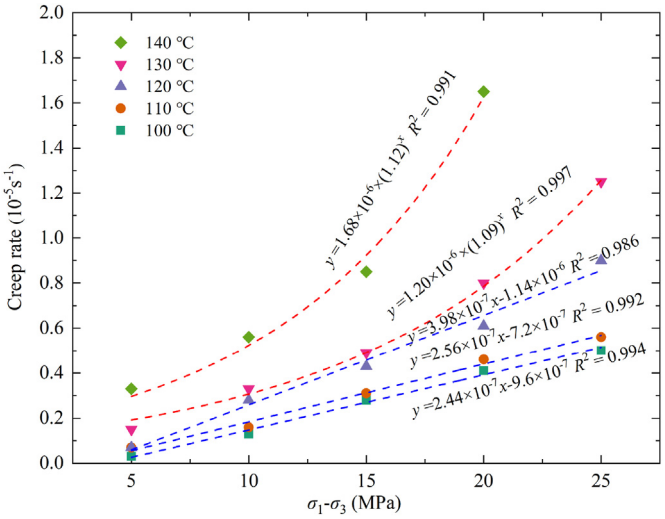

Fig. 8. Creep rate at steady state under different conditions.

An extension of the one-dimensional model to the 3D model entails the following relationships between $K(T)$, $G(T)$, and $E(T)$:

$$\left.\begin{aligned} G(T) &= \frac{E(T)}{2(1+\mu)} \\ K(T) &= \frac{E(T)}{3(1-2\mu)} \end{aligned}\right\} \tag{18}$$

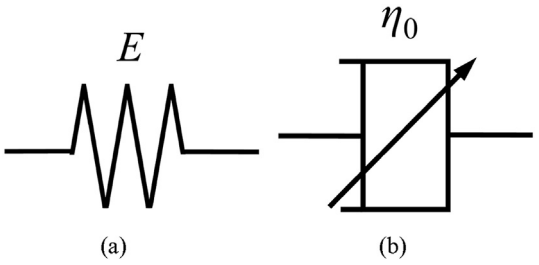

Fig. 10. Basic mechanical elements: (a) Hooke's body; and (b) Abel dashpot.

Hence, the strain of Hooke's body can be expressed by a 3D form:

$$\varepsilon_{ij}^{\mathrm{e}} = \frac{S_{ij}}{2G(T)} + \frac{\delta_{ij}\sigma_{\mathrm{m}}}{3K(T)} \tag{19}$$

The rock deformation in the steady creep phase is principally manifested by shear deformation, assuming that the volume change is elastic. Therefore, the first Abel dashpot has the following 3D constitutive relation:

$$\varepsilon_{ij}^{\mathrm{ve}} = \frac{S_{ij}}{2G_0(T)} \frac{t^{\gamma}}{\Gamma(\gamma+1)} \quad (0 \le \gamma \le 1) \tag{20}$$

where $G_0(T)$ is the shear modulus of the first Abel dashpot considering the effect of temperature T, GPa s^{γ}.

Similarly, the second Abel dashpot has the following 3D constitutive relation:

$$\varepsilon_{ij}^{\mathrm{vp}} = \frac{S_{ij}}{2G_1(T,\sigma)} \frac{t_1^{\gamma}}{\Gamma(\gamma+1)} \quad (0 \le \gamma \le 1) \tag{21}$$

Where $G_1(T,\sigma)$ is the shear modulus of second Abel dashpot at temperature T, which is affected by mechanical damage, GPa s^{γ}.

Hence, the creep equation in three-dimensions is defined as follows:

$$\varepsilon_{ij} = \begin{cases} \dfrac{S_{ij}}{2G(T)} + \dfrac{\delta_{ij}\sigma_{\mathrm{m}}}{3K(T)} + \dfrac{S_{ij}}{2G_0(T)} \dfrac{t^{\gamma}}{\Gamma(\gamma+1)} & (\varepsilon < \varepsilon_{\mathrm{s}}) \\ \dfrac{S_{ij}}{2G(T)} + \dfrac{\delta_{ij}\sigma_{\mathrm{m}}}{3K(T)} + \dfrac{S_{ij}}{2G_0(T)} \dfrac{t^{\gamma}}{\Gamma(\gamma+1)} + \dfrac{S_{ij}}{2G_1(T,\sigma)} \dfrac{t_1^{\gamma}}{\Gamma(\gamma+1)} & (\varepsilon \ge \varepsilon_{\mathrm{s}}) \end{cases} \tag{22}$$

The creep experiments are conducted under the pseudo-triaxial conditions which have the same confining pressure:

$$\sigma_2 = \sigma_3 \tag{23}$$

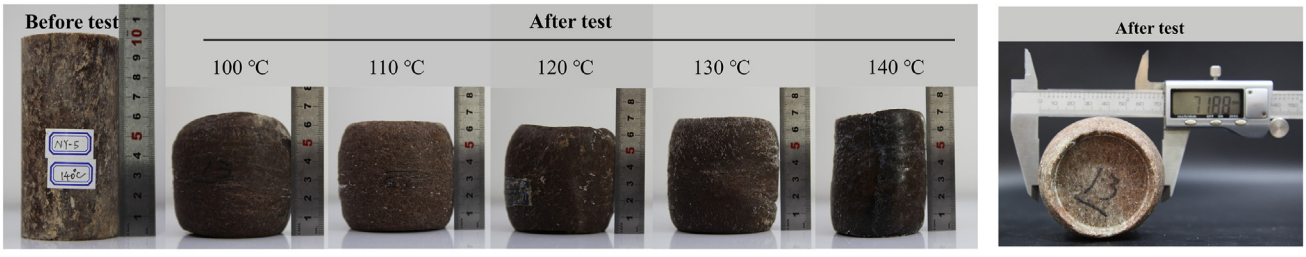

Fig. 9. Comparison of deformation morphology of impurity salt rock under different temperature conditions: (a) Axial direction; and (b) Radial direction.

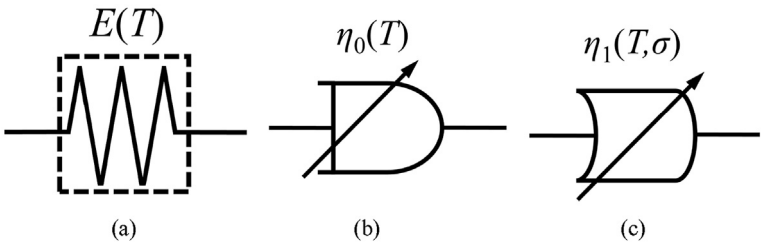

Fig. 11. Modified mechanical elements: (a) Hooke's body; (b) 1st Abel dashpot; and (c) 2nd Abel dashpot.

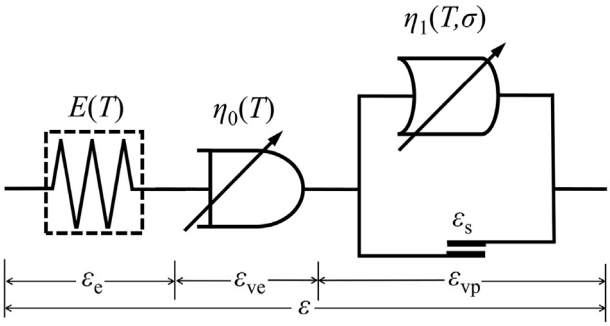

Fig. 12. Fractional derivative model incorporates thermal and mechanical effect.

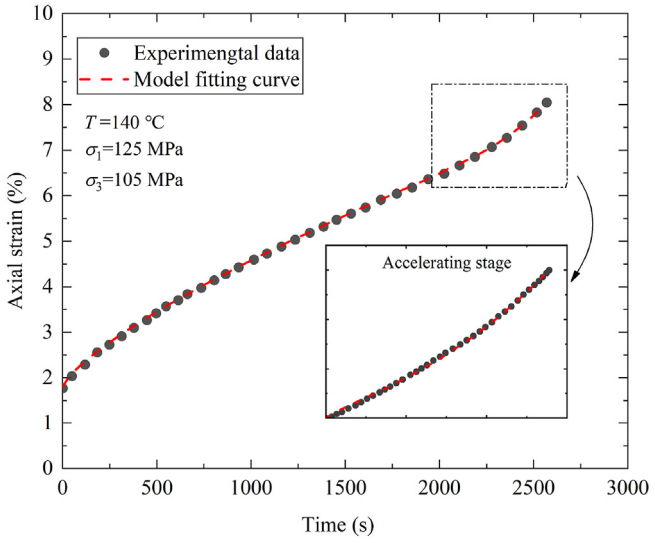

Fig. 13. Comparison of fitting results and experimental data at ($\sigma_1-\sigma_3$ = 20 MPa, T = 140 °C).

$$\sigma_m = \frac{1}{3}(\sigma_1+\sigma_2+\sigma_3) = \frac{1}{3}(\sigma_1+2\sigma_3) \tag{24}$$

$$i = j = 1, \delta_{ij} = 1 \tag{25}$$

$$S_{11} = \sigma_1 - \sigma_m = \frac{2}{3}(\sigma_1-\sigma_3) \tag{26}$$

Substituting Eqs. (24)–(26) into Eq. (22), the triaxial creep equation considering thermal and mechanical damage can be obtained by

Table 2
Parameters and magnitude of the creep model fitting.

Parameter	Value	Parameter	Value
Shear modulus (G, GPa)	1.124	Fractional derivative order (γ)	0.75
Shear modulus (G_0, GPa s^{γ})	1.276	Temperature effect constant (α)	0.506
Shear modulus (G_1, GPa s^{γ})	3.449	Temperature effect constant (β)	−0.098
Bulk modulus (K, GPa)	0.057	Parameter of viscosity coefficient (ω, s^{-1})	0.001

$$\varepsilon_{11} = \begin{cases} \dfrac{\sigma_1-\sigma_3}{3G(T)} + \dfrac{\sigma_1+2\sigma_3}{9K(T)} + \dfrac{\sigma_1-\sigma_3}{3G_0(T)\Gamma(\gamma+1)}t^{\gamma} & (\varepsilon<\varepsilon_s) \\ \dfrac{\sigma_1-\sigma_3}{3G(T)} + \dfrac{\sigma_1+2\sigma_3}{9K(T)} + \dfrac{\sigma_1-\sigma_3}{3G_0(T)\Gamma(\gamma+1)}t^{\gamma} + \dfrac{\sigma_1-\sigma_3}{3G_1(T,\sigma)\Gamma(\gamma+1)}t_1^{\gamma} & (\varepsilon\geq\varepsilon_s) \end{cases} \tag{27}$$

4.4. Model validation

For verification, the creep duration curve under the condition of σ_1 = 125 MPa and σ_3 = 105 MPa at temperature 140 °C was selected to determine whether the constitutive model is applicable. Using the standard particle swarm optimization (SPSO) algorithm, the creep parameters of the model are determined (Lyu et al., 2021). As shown in Fig. 13, the fitting curve and experimental data are compared. The parameters are listed in Table 2. It is shown that the novel creep constitutive model is reasonably consistent with experimental data and that the results of the fitting are highly

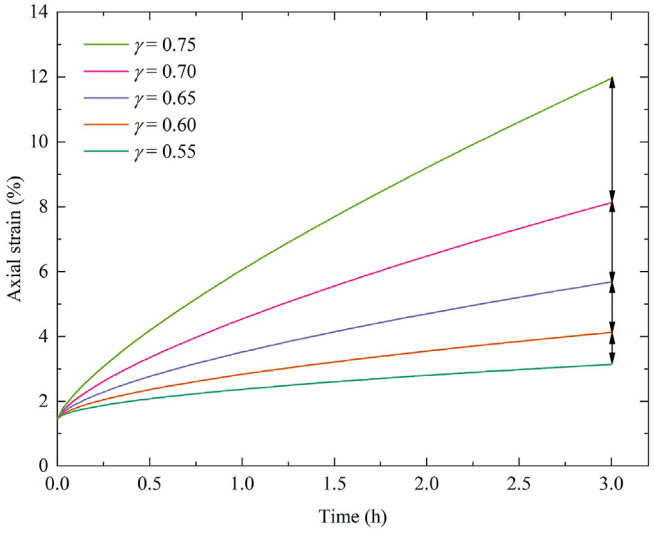

Fig. 14. Comparison of the creep strain with different fractional derivative order.

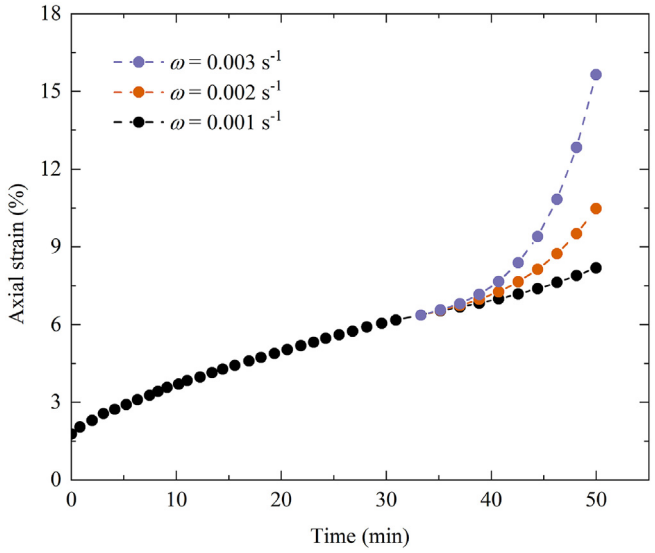

Fig. 15. Comparison of the creep strain with different Parameter of viscosity coefficient.

correlated. Overall, the model proposed above can accurately describe the creep strain evolution under the effect of ultra-high temperature and pressure.

To further analyze the key parameters in the constitutive equation that affect the evolution of the creep curve, we take different values for the fractional derivative order γ and the parameter of viscosity coefficient ω respectively, based on the condition of σ_1-$\sigma_3 = 20$ MPa and $T = 140$ °C. The influence mechanism of each parameter can be clarified through the sensitivity analysis. As shown in Fig. 14, five fractional derivative orders ranging from 0.55 to 0.75 are selected to compare the influence of order on the development of creep curve. It is seen that the same increment of order leads to different increments of the total strain as the order increases, and the strain increment at different order raises as the order increases. With regard to the parameter of viscosity coefficient, it is evident from Fig. 15 that as the parameter increases, the slope of creep curve increases and the growth of strain accelerates. This observation suggests that the viscosity coefficient parameter can accurately describe the development law of strain damage over time.

5. Conclusions

The novel triaxial constitutive creep model has been proposed and verified based on the creep experiments conducted on deep salt under varying temperatures and pressures. The main conclusions can be drawn as follows:

(1) Triaxial unloading creep experiments have been carried out at elevating temperature conditions for impurity salt samples. The creep deformation grows with increasing temperature and deviatoric stress. The accelerating creep occurs in all specimens after the temperature reaches 130 °C, and higher temperature is beneficial to the earlier occurrence of accelerating creep.

(2) The mechanical elements considering thermal and mechanical effect has been constructed and substituted into elastic-plastic continuum model. Based on the fractional derivatives and the corresponding modification, we have proposed an innovative triaxial constitutive creep model.

(3) The SPSO method has been adopted to validate the developed triaxial creep model with experimental data and the corresponding key parameters of the model have been determined. It has been proved that this model can accurately represent the creep behavior of deep-buried salt under thermal and mechanical effect.

Declaration of competing interest

The authors declare that they have no known competing financial interests or personal relationships that could have appeared to influence the work reported in this paper.

Acknowledgments

This research was financially supported by the Scientific and technological research projects in Sichuan province (Grant Nos. 2022YFSY0007 and 2021YFH0010), and the National Scientific Science Foundation of China (Grant No. U20A20266).

References

Blanco-Martín, L., Wolters, R., Rutqvist, J., Lux, K.H., Birkholzer, J.T., 2016. Thermal–hydraulic–mechanical modeling of a large-scale heater test to investigate rock salt and crushed salt behavior under repository conditions for heat-generating nuclear waste. Comput. Geotech. 77, 120–133.
Cai, M.F., Duo, J., Chen, X.S., et al., 2021. Development strategy for co-mining of the deep mineral and geothermal resources. Chin. J. Eng. Sci. 23 (6), 43–51 (in Chinese).
Chen, H.J., Xu, W.Y., Wang, W., Wang, R.B., Shi, C., 2013. A nonlinear viscoelastic-plastic rheological model for rocks based on fractional derivative theory. Int. J. Mod. Phys. B 27 (25), 1350149.
Chen, J., Lu, D., Wu, F., Fan, J.Y., Liu, W., 2019. A non-linear creep constitutive model for salt rock based on fractional derivatives. Therm. Sci. 23 (Suppl. 3), 773–779.
Chen, L., et al., 2014. A damage-mechanism-based creep model considering temperature effect in granite. Mech. Res. Commun. 56, 76–82.
Cheng, W., Jiang, G.S., Li, X.D., Zhou, Z.D., Wei, Z.J., 2019. A porochemothermoelastic coupling model for continental shale wellbore stability and a case analysis. J. Pet. Sci. Eng. 182, 106265.
De Las Cuevas, C., 1997. Pore structure characterization in rock salt. Eng. Geol. 47 (1-2), 17–30.
Dusseault, M.B., Maury, V., Sanfilippo, F., Santarelli, F.J., 2004. Drilling around salt: risks, stresses, and uncertainties. In: Gulf Rocks – 6th North America Rock Mech. Symp(NARMS). GulfRocks, (Houston, TX).
Feng, X.T., Haimson, B., Li, X.C., et al., 2019. ISRM Suggested Method: determining deformation and failure characteristics of rocks subjected to true triaxial compression. Rock Mech. Rock Eng. 52 (6), 2011–2020.
Feng, Y.Y., Yang, X.J., Liu, J.G., Chen, Z.Q., 2021. A new fractional Nishihara-type model with creep damage considering thermal effect. Eng. Fract. Mech. 242, 107451.
Hu, Q.Z., Feng, X.T., Zhou, H., 2009. Study of creep model of rock salt with thermal damage considered. Yantu Lixue/Rock Soil Mech. 30 (8), 2245–2248 (in Chinese).
Kumari, W.G.P., et al., 2017. Mechanical behaviour of Australian Strathbogie granite under in-situ stress and temperature conditions: an application to geothermal energy extraction. Geothermics 65, 44–59.
Li, W.J., Zhu, C., Yang, C.H., Duan, K., Hu, W.R., 2018. Experimental and DEM investigations of temperature effect on pure and interbedded rock salt. J. Nat. Gas Sci. Eng. 56, 29–41.
Liang, C., Liu, J.F., Chen, Z.W., Lu, G.D., Lyu, C., Ren, Y., 2022. Study on salt rock creep characteristics of wellbore under high temperature and high pressure. J. Porous Media 25 (3), 51–69.
Lyu, C., Liu, J.F., Ren, Y., Liang, C., Liao, Y.L., 2021. Study on very long-term creep tests and nonlinear creep-damage constitutive model of salt rock. Int. J. Rock Mech. Min. Sci. 146, 104873.
Lyu, C., Liu, J.F., Ren, Y., Liang, C., Zeng, Y., 2022. Mechanical characteristics and permeability evolution of salt rock under thermal-hydro-mechanical (THM) coupling condition. Eng. Geol. 302, 106633.
Peng, G., Chen, Z.Q., Chen, J.R., 2018. Research on rock creep characteristics based on the fractional calculus meshless method. Adv. Civ. Eng. 2018, 1–6.
Soppe, W.J., Donker, H., García Celma, A., Prij, J., 1994. Radiation-induced stored energy in rock salt. J. Nucl. Mater. 217 (1-2), 1–31.
Taheri, S.R., Pak, A., Shad, S., Mehrgini, B., Razifar, M., 2020. Investigation of rock salt layer creep and its effects on casing collapse. Int. J. Min. Sci. Technol. 30 (3), 357–365.
Tang, M.M., Wang, Z.Y., Ding, G.S., Ran, L.N., 2010. Creep property experiment and constitutive relation of salt-mudstone interlayer. J. China Coal Soc. 35 (1), 42–45 (in Chinese).

Tao, J., Yang, X.G., Li, H.T., Zhou, J.W., Fan, G., Lu, G.D., 2020. Effects of in-situ stresses on dynamic rock responses under blast loading. Mech. Mater. 145, 103374, 1–11.
Wang, H., et al., 2019. Quantitative determination of the brittle–ductile transition characteristics of caprocks and its geological significance in the Kuqa depression, Tarim Basin, western China. J. Pet. Sci. Eng. 173, 492–500.
Wang, J.B., Liu, X.R., Wang, T.H., 2015. A nonlinear creep model for rocks based on modified fractional viscous body. J. Cent. South Univ. Sci. Technol. 46 (4), 1461–1467 (in Chinese).
Wang, J.B., Zhang, Q., Song, Z.P., Zhang, Y.W., 2020. Creep properties and damage constitutive model of salt rock under uniaxial compression. Int. J. Damage Mech. 29 (6), 902–922.
Wang, L.C., Zhu, Z.Q., Lei, J.W., Zhang, S.H., Long, W., Shu, B., 2021. Mechanical responses to wellbore instability of crystalline rocks in scientific deep well during thermo-mechano coupling. J. Cent. South Univ. Sci. Technol. 52 (2), 465–477 (in Chinese).
Wu, C., Liu, J.F., Xu, H.N., Wu, F., Zhuo, Y., Wang, L., 2017. Study on creep properties of salt rock with Impurities during triaxial creep Test. Adv. Eng. Sci. 49 (Suppl. 2), 165–172 (in Chinese).
Wu, F., Gao, R.B., Liu, J., Li, C.B., 2020a. New fractional variable-order creep model with short memory. Appl. Math. Comput. 380, 125278.
Wu, F., Liu, J., Zou, Q.L., Li, C.B., Chen, J., Gao, R.B., 2021. A triaxial creep model for salt rocks based on variable-order fractional derivative. Mech. Time-Dependent Mater. 25 (1), 101–118.
Wu, F., Zhang, H., Zou, Q.L., Li, C.B., Chen, J., Gao, R.B., 2020b. Viscoelastic-plastic damage creep model for salt rock based on fractional derivative theory. Mech. Mater. 150, 103600.
Wu, F., Zhou, X.H., Ying, P., Li, C.B., Zhu, Z.M., Chen, J., 2022. A study of uniaxial acoustic emission creep of salt rock based on improved fractional-order derivative. Rock Mech. Rock Eng. 55 (3), 1619–1631.
Xi, B.P., Zhao, Y.S., Xu, S.G., 2008. Study on coupled thermo-mechanical creep properties of bedded rock salt. Chin. J. Rock Mech. Eng. 27 (1), 90–96 (in Chinese).
Xi, B.P., Zhao, Y.S., Zhao, Y.L., Xu, S.G., 2007. Study on creep property of rock salt with mudstone interlayer. Chin. J. Undergr. Space Eng. 3 (1), 23–26 (in Chinese).
Xie, H.P., Gao, F., Ju, Y., 2015. Research and development of rock mechanics in deep ground engineering. Chin. J. Rock Mech. Eng. 34 (11), 2161–2178 (in Chinese).
Xie, H.P., Liu, J.F., Ju, Y., Li, J., Xie, L.Z., 2011. Fractal property of spatial distribution of acoustic emissions during the failure process of bedded rock salt. Int. J. Rock Mech. Min. Sci. 48 (8), 1344–1351.
Xu, H., Yang, X.G., Zhang, J.H., Zhou, J.W., Tao, J., Lu, G.D., 2020. A closed-form solution to spherical wave propagation in triaxial stress fields. Int. J. Rock Mech. Min. Sci. 128, 104266.
Xu, X.L., Karakus, M., 2018. A coupled thermo-mechanical damage model for granite. Int. J. Rock Mech. Min. Sci. 103, 195–204.
Yang, J.X., Fall, M., 2021. A two-scale time dependent damage model for preferential gas flow in clayey rock materials. Mech. Mater. 158, 103853.
Yang, J.X., Fall, M., Guo, G.L., 2020. A three-dimensional hydro-mechanical model for simulation of dilatancy controlled gas flow in anisotropic claystone. Rock Mech. Rock Eng. 53 (9), 4091–4116.
Yang, S.Q., Ranjith, P.G., Jing, H.W., Tian, W.L., Ju, Y., 2017. An experimental investigation on thermal damage and failure mechanical behavior of granite after exposure to different high temperature treatments. Geothermics 65, 180–197.
Zhang, G.M., Li, Y.P., Yang, C.H., Daemen, J.J.K., 2014. Stability and tightness evaluation of bedded rock salt formations for underground gas/oil storage. Acta Geotech 9 (1), 161–179.
Zhang, L., et al., 2021. A triaxial creep model for deep coal considering temperature effect based on fractional derivative. Acta Geotech 17 (5), 1739–1751.
Zhang, Q.X., Liu, J.F., Wang, L., et al., 2020. Impurity effects on the mechanical properties and permeability characteristics of salt rock. Energies 13 (6), 1366.
Zhang, S.L., Liang, W.G., Xiao, N., Zhao, D.S., Li, J., Li, C., 2022. A fractional viscoelastic-plastic creep damage model for salt rock considering temperature effect. Chin. J. Rock Mech. Eng. 41 (Suppl. 2), 3198–3209 (in Chinese).
Zhou, H.W., Wang, C.P., Han, B.B., Duan, Z.Q., 2011. A creep constitutive model for salt rock based on fractional derivatives. Int. J. Rock Mech. Min. Sci. 48 (1), 116–121.
Zhou, H.W., Wang, C.P., Mishnaevsky, L., Duan, Z.Q., Ding, J.Y., 2013. A fractional derivative approach to full creep regions in salt rock. Mech. Time-Dependent Mater. 17 (3), 413–425.
Zhu, Y.G., Liu, Q.S., Kang, Y.S., Liu, K.D., 2011. Study of creep damage constitutive relation of granite considering thermal effect. Chin. J. Rock Mech. Eng. 30 (9), 1882–1888 (in Chinese).

Dr. Jianfeng Liu obtained his PhD from College of Water Resources and Hydropower, Sichuan University, China, in 2009. He was selected as a Distinguished Professor of Changjiang Scholar Program as well as Academic and Technical leader of Sichuan Province in 2020. In 2022, he was granted the Science and Technology Award (Youth Innovation) by Ho Leung Ho Lee Foundation. He has been engaged in the basic theory and engineering practice research on deep rock mass mechanics. He has published more than 130 journal papers.